NOTICE
This report was prepared as an account of work sponsored by the United States Government. Neither the United States nor the United States Energy Research and Development Administration, nor any of their employees, nor any of their contractors, subcontractors, or their employees, makes any warranty, express or implied, or assumes any legal liability or responsibility for the accuracy, completeness or usefulness of any information, apparatus, product or process disclosed, or represents that its use would not infringe privately owned rights.

PIONIC INSTABILITIES IN HIGH-ENERGY HEAVY ION COLLISIONS*

Miklos Gyulassy
Nuclear Science Division, Lawrence Berkeley Lab,
University of California, Berkeley CA 94720

I. Introduction

Heavy ion scattering at energies 0.2 - 2.0 GeV/nucleon provides a unique opportunity to study properties of nuclear systems far outside the realm of conventional nuclear physics. In such collisions nuclear matter could be compressed to densities $\rho \sim (2\text{-}4)\rho_0$ where $\rho_0 \approx 0.17\ \text{fm}^{-3} \approx m_\pi^3/2$. At these densities collective phenomena may become important, leading to phase transitions in the nuclear system. Indeed, model calculations[1,2] for cold nuclear systems (T = 0) indicate that above some critical density $\rho_c \sim (1\text{-}2)\,\rho_0$, the pion field acquires a finite ground state expectation value. This phase transition, called pion condensation, would lead to a spin-isospin lattice, $\langle \psi^+(x)\sigma_i\,\tau_\alpha\psi(x)\rangle = \chi_{i\alpha}\exp(i\,\tilde{k}_c\tilde{x})$ with wavelength $2\pi/k_c \sim (3 - 5)\ m_\pi^{-1}$ in the nuclear system. While densities $\rho > \rho_c$ could easily be reached in heavy ion collisions, these high densities are produced only at the price of high excitation energies E^* as well. For these collisions, E^* is typically on the order of 50-100 MeV/nucleon.

One may expect that such high excitation energies would tend to inhibit, if not eliminate, any possible collective instabilities involving the coherent interaction of many nucleons. This is certainly the case if the system has come to thermal equilibrium. In that case E^* is converted into random motion of the nucleons, and as E^* increases, so does the disorder in the system. Long range correlations will then eventually be destroyed as E^* increases. However, in non-equilibrium systems E^* can be tied up in ordered motion, e.g. half of the nucleons have momentum $\approx \tilde{p}_{cm}$ while the other half have momentum $\approx -\tilde{p}_{cm}$. In this case, collective instabilities may actually be enhanced as E^* increases!

The most familiar example that illustrates this dependence on E^* is colliding plasma beams.[3] Below some critical velocity v_c all plasmon modes are stable. However, as the relative velocity v increases beyond v_c, certain plasmon modes become unstable. This instability leads then to the growth of strong, collective electric fields with a growth rate that increases as a function of $v - v_c$. The instability exists, however, only in the non-equilibrium stage of the collision. As the plasma beams thermalize through the interactions with these collective fields, the plasmon instabilities disappear.

In heavy ion collisions we look for analogous collective instabilities. The analogue of the electric field in nuclear systems is the pion field. The program then is

(1) to determine whether pionic instabilities can exist at the densities and excitation energies expected in heavy ion collisions,
(2) to calculate growth rates of unstable pion modes, and

DISTRIBUTION OF THIS DOCUMENT IS UNLIMITED

(3) to determine the effect such instabilities would have on the dynamics in heavy ion collisions.

II. Unstable pion modes in excited nuclear matter

The existence of pionic instabilities in excited nuclear matter was first investigated for thermal equilibrated systems.[4] The critical temperature $T_{crit}(\rho)$ is shown in Fig. I. For a given density ρ, nuclear matter is unstable with respect to pion condensation for $T < T_{crit}(\rho)$. The details of the calculation of T_{crit} are given in Ref. (4). The paths AB and BC follow the hydrodynamic compression and decompression of nuclear matter in heavy ion collisions. Curve AB is taken from Ref. (5) and corresponds to the solution of the Rankine shock equation for compressibility K = 300 MeV including also Δ_{33} isobar production. Curve BC is a guess for the decompression path noting that as the system expands, the compression energy E_{comp} at point B is converted into thermal energy E_{therm} by point C. Estimates in Ref. (5) indicate $E_{comp}/E_{therm} \sim 1/10$. As the system expands it also cools down through evaporation of nucleons. Beyond point C the system becomes so diffuse that local thermal equilibration can no longer be assumed. The important point to note in Fig. I is that for the maximum densities, ρ_B, expected at these energies (see Fig. 14 of Ref. (5)), the temperature T_B is less than $T_{crit}(\rho_B)$. Therefore, pion condensation is likely to occur in spite of the relatively high temperatures in heavy ion collisions.

We turn now to the question of whether pionic instabilities can also occur during the non-equilibrium stage of the collision. We are then looking for the pion field analogue of the two beam instability in plasmas.[3] The following considerations motivate our study of non-equilibrium systems. First, the stopping distance λ_L of a nucleon in nuclear matter is estimated to be $\lambda_L \gtrsim 4$ fm for $E_{lab} \gtrsim 1$ GeV. The thermalization time τ_{th} is then roughly $\tau_{th} \sim 2\lambda_L/v_{rel} \sim 2 - 3 \times 10^{-23}$ sec. Therefore, a substantial fraction of the total interaction time $\tau_{int} \sim 2 R_{target}/v_{rel} \sim 3 - 6 \times 10^{-23}$ sec involves non-equilibrium dynamics. Second, the effects of collective instabilities on the dynamics may in fact be greatest during that non-equilibrium stage of the collision. Depending on the ratio of the growth rate Γ_{col} of collective fields to the two body scattering rate Γ_{scat}, the dynamics will be categorized[7] either by (1) wave-particle interactions as in collisionless plasmas or (2) particle-particle interactions as in hydrodynamics. We discuss this point further in section IV.

As a model of the initial, non-equilibrium momentum distribution of nucleons we take[7]

$$n(\tilde{p}) = n_o(\tilde{p} + \tilde{p}_{cm}) + n_o(\tilde{p} - \tilde{p}_{cm}) \tag{1}$$

with $n_o(\tilde{p}) = \theta(p_F - |\tilde{p}|)$ as illustrated in Fig. II. To look for pionic instabilities, we search for complex poles of the pion propagator $\Delta(\omega,\tilde{k})$.

In nuclear matter, $\Delta(\omega,\tilde{k})$ differs from the free space propagator $\Delta_0(\omega,\tilde{k}) = (\omega^2 - k^2 - 1 + i\varepsilon)^{-1}$ because of the polarizability of the medium as shown in Fig. IIIa. In terms of the polarization operator[1,2] $\Pi(\omega,\tilde{k})$,

$$\Delta^{-1} = \Delta_0^{-1} - \Pi \quad . \tag{2}$$

The dominant interactions that must be included in Π are[1,2] (1) the P-wave πNN interaction, (2) the P-wave $\pi N\Delta$ resonance interaction, and (3) hard core NN, $N\Delta$ and $\Delta\Delta$ interactions that lead to nucleon and isolar correlations. In symmetric nuclear matter the S-wave πN interaction does not contribute in lowest order.

The πNN interaction leads to a contribution Π_{NN} to the polarization operator due to the excitation of nucleon particle-hole states. We consider here only spin-isospin saturated nuclear systems having reflection symmetric momentum distributions ($n(\tilde{p}) = n(-\tilde{p})$). In that case[1,2,7]

$$\Pi_{NN}(\omega,\tilde{k}) = -i\,4\,f^2k^2\,F_\pi^2(\omega,\tilde{k}) \int \frac{d^4p}{(2\pi)^4}\; S_N(p)\; S_N(p+k) \tag{3a}$$

$$= 4f^2k^2F_\pi^2(\omega,\tilde{k}) \int \frac{d^3p}{(2\pi)^3}\; n(\tilde{p})\;\; (1-n(\tilde{p}+\tilde{k}))$$

$$\times \left\{ \frac{1}{\omega-\omega_{pk}+i\varepsilon} - \frac{1}{\omega+\omega_{pk}-i\varepsilon} \right\} \tag{3b}$$

$$= \frac{1}{\pi}\int_{-\infty}^{\infty} d\omega'\;\; I_{NN}(\omega',\tilde{k}) \;\; \left\{ \frac{1}{\omega-\omega'+i\varepsilon} - \frac{1}{\omega+\omega'-i\varepsilon} \right\} \tag{3c}$$

The non-relativistic nucleon propagator S_N is

$$S_N(p_0,\tilde{p}) = \frac{n(\tilde{p})}{p_0-\varepsilon_N(\tilde{p})-i\varepsilon} + \frac{(1-n(\tilde{p}))}{p_0-\varepsilon_N(\tilde{p})+i\varepsilon} \quad , \tag{4}$$

with $\varepsilon_N(\tilde{p})$ being the single particle energies. In eq. (3b), $\omega_{pk} = \varepsilon_N(\tilde{p}+\tilde{k}) - \varepsilon_N(\tilde{p})$. The πNN coupling $f^2 \approx m_\pi^{-2}$ and the form factor $F_\pi(\omega,\tilde{k})$ is taken to be

$$F_\pi(\omega,k) = (\Lambda^2 - 1)/(\Lambda^2 - \omega^2 + k^2) \tag{5}$$

with $\Lambda \approx M_N/m_\pi = 6.7$. Dipole form factors[8] with $\Lambda \approx 8.3$ differ by $< 10\%$ for the ω,k considered here.

In the dispersion relation form, eq. (3c), I_{NN} measures the discontinuity of Π_{NN} across cuts in the upper and lower half ω plane. These cuts arise because a pion of momentum $\tilde{k}$ and energy $\omega = \omega_{pk}$ can decay into a one particle - one hole excitation conserving energy-momentum.

Through the resonant $\pi N\Delta$ interaction, a pion can excite not only nucleon particle-hole states via Π_{NN} but also Δ-particle-nucleon hole states via $\Pi_{N\Delta}$, where

$$\Pi_{N\Delta}(\omega,\tilde{k}) = -i\, f_\Delta^2 k^2 F_\pi^2(\omega,\tilde{k}) \int \frac{d^4p}{(2\pi)^4} \left\{ S_N(p)\, S_\Delta(p+k) + S_N(p)\, S_\Delta(p-k) \right\} \quad . \tag{6}$$

In. eq. (6), the Δ intermediate state is included in both s and u channels (direct + cross graphs). The $\pi N\Delta$ coupling (including spin-isospin factors) is[1,7] $f_\Delta^2 \approx 8m_\pi^{-2}$. The form factor is taken to be the same as the πNN form factor, eq. (5), as suggested by fits to $\nu p \to \mu^- \Delta^{++}$ data.[9] For the Δ propagator we take

$$S_\Delta(p_o,\tilde{p}) = (p_o - \varepsilon_\Delta(\tilde{p}) - i\,\mathrm{Im}\,\Sigma_\Delta(p_o,\tilde{p}) + i\varepsilon)^{-1} \quad , \tag{7}$$

where the Δ self energy Σ_Δ is included to account for the finite Δ width. The real part of Σ_Δ is absorbed into $\varepsilon_\Delta(\tilde{p})$, which we approximate by $\varepsilon_\Delta(\tilde{p}) = m_\Delta + p^2/2m_\Delta$, with $m_\Delta = 8.8\, m_\pi$. $\mathrm{Im}\,\Sigma_\Delta \neq 0$ when the Δ can decay to a free pion and nucleon, i.e., when $p_o^2 - p^2 \gtrsim (m_N+m_\pi)^2$. We ignore the relatively small modification of Σ_Δ due to the presence of nuclear matter[10] and take the free space value of Σ_Δ. The effect of $\mathrm{Im}\,\Sigma_\Delta$ is to smear out the Δ mass. We therefore write

$$S_\Delta(p) = \int_0^\infty dm\, \rho_\Delta(m)\, S_\Delta(p;m) \quad , \tag{8}$$

where

$$S_\Delta(p,m) \equiv (p_o - m - \frac{\tilde{p}^2}{2m_\Delta} + i\varepsilon)^{-1} \quad . \tag{9}$$

Then computing $\mathrm{Im}\, S_\Delta$ from eqs. (7,8,9), the Δ spectral density is seen to be

$$\rho_\Delta(m) = -\frac{1}{\pi}\, \mathrm{Im}\, S_\Delta(p_o = m + p^2/2m_\Delta\ ,\ \tilde{p}) = \frac{c_\Delta\, \gamma_\Delta(m)}{(m-m_\Delta)^2 + \gamma_\Delta^2(m)} \quad , \tag{10}$$

The $\tilde{p}$ dependence of ρ_Δ and γ_Δ in eqs. (8,10) can be neglected because of

the small Δ width $\Gamma_\Delta = 2\gamma_\Delta(m_\Delta) = 120$ MeV $\Rightarrow \gamma_\Delta/m_\Delta << 1$. Then $\gamma_\Delta(m) \approx$ - Im $\Sigma_\Delta(m^2)$. For the moment $c_\Delta = 1/\pi$. We note that canonical anti-commutation stations for the Δ field require that

$$\int_0^\infty \rho_\Delta(m)dm = 1 \quad . \tag{11}$$

As long as $(p_o,\tilde{p})$ in eq. (8) is not near threshold $(m = m_N + m_\pi)$, a good approximation for $S_\Delta(p)$ is obtained by taking $\rho_\Delta(m)$ to be Lorenzian, i.e., setting

$$\gamma_\Delta(m) = \theta(m-m_N-m_\pi)\ \theta(2m_\Delta-m_N-m_\pi-m)\ \gamma_\Delta(m_\Delta) \quad . \tag{12}$$

The upper mass cut off is chosen to give a symmetric weight of masses in eq. (8) about m_Δ. Larger mass are estimated to contribute only $\sim$10% to the sum rule, eq. (11), as a result of the small Δ width, γ_Δ=.43 m_π. With eq. (12), c_Δ in eq. (10) is then determined so that eq. (11) is satisfied.

With eqs. (6,8) we then get for $\Pi_{N\Delta}$

$$\Pi_{N\Delta}(\omega,\tilde{k}) = f_\Delta^2 k^2 F_\pi^2(\omega,\tilde{k}) \int_0^\infty dm\ \rho_\Delta(m) \left[U_{N\Delta}(\omega,\tilde{k};m) + U_{N\Delta}(-\omega,-\tilde{k};m) \right] \tag{13}$$

where the NΔ Lindhard function is

$$U_{N\Delta}(\omega,\tilde{k};m) = \int \frac{d^3p}{(2\pi)^3} \frac{n(\tilde{p})}{\omega + (m_N-m) + \frac{p^2}{2m_N} - \frac{(\tilde{p}+\tilde{k})^2}{2m_\Delta} + i\varepsilon} \quad . \tag{14}$$

Note, eq. (13) reduces to eq. (4.4) of Ref. (7) when $\rho_\Delta(m) = \delta(m - m_\Delta)$. The inclusion of the finite Δ width will be important when we estimate on-shell pion production rates in section III. As in eq. (3c), it is convenient to write

$$\Pi_{N\Delta}(\omega,\tilde{k}) = \frac{1}{\pi} \int_{-\infty}^{\infty} d\omega'\ I_{N\Delta}(\omega',\tilde{k}) \left\{ \frac{1}{\omega-\omega'+i\varepsilon} - \frac{1}{\omega+\omega'-i\varepsilon} \right\} \quad . \tag{15}$$

Expressions for scattering rates become more compact in terms of I_{NN} and $I_{N\Delta}$ in section III.

Note that $\Pi_{NN} + \Pi_{N\Delta}$ is the pion-nucleon forward scattering amplitude summed over all the nucleons in the medium; Π_{NN} is the Born term involving only a single nucleon intermediate state while $\Pi_{N\Delta}$ is a model for the contribution from πN continuum intermediate states. The strong distortion of the πN continuum near the Δ_{33} resonance is described by $\rho_\Delta(m)$ in eq. (10). The propagation of a pion in the medium via eq. (2) with $\Pi = \Pi_{NN} + \Pi_{N\Delta}$ then consists of a series of elastic πN scatterings. However, in this multiple scattering series only one pion exchange (OPE) is included between successive collisions. Clearly, multiple meson exchange must also be included, especially the exchange of vector mesons ρ,ω that give rise to the hard core repulsion between nucleons. These interactions tend to keep nucleons apart and lead to short range correlations in the medium.

Such correlations are included in Π via an effective interaction $G_c(\tilde{k})$ as illustrated in Fig. IIIb. The correlated polarization operator is then[2,7]

$$\Pi(\omega,\tilde{k}) = \frac{\Pi_{NN}(\omega,\tilde{k}) + \Pi_{N\Delta}(\omega,\tilde{k})}{1 - G_c(k)\,(\Pi_{NN}(\omega,\tilde{k}) + \Pi_{N\Delta}(\omega,\tilde{k}))} \quad . \qquad (16)$$

Detailed calculations[11] show that $G_c(k) \approx g/k^2$, where the correlation parameter $g = 0.5 \pm 0.1$. This form of G_c follows[7] when the πNN and $\pi N\Delta$ vertices are included in the definition of Π_{NN} and $\Pi_{N\Delta}$ as in eqs. (3,13). The parameter g measures the strength of the repulsive hard core NN, $N\Delta$, and $\Delta\Delta$ interactions. A value of $g = 1/3$ would just remove the attractive $\delta(\tilde{x})$ part of the OPE potential.[2] A value of $g = 2/3$ would then reverse the sign of that $\delta(\tilde{x})$ part of OPE.

Evaluating eq. (16) for the system specified by eq. (1), the singularities of $\Delta(\omega,\tilde{k})$ in eq. (2) and hence the pion spectrum can be determined. These singularities are analyzed in detail in Ref. 7. To look for unstable pion modes, we search for complex roots $\omega = \mathrm{Re}\,\omega_c(\tilde{k}) + i\gamma(\tilde{k})$ of $\Delta^{-1}(\omega,\tilde{k}) = 0$. As discussed in Ref. (7), $\gamma(\tilde{k})$ can be interpreted as the rate for spontaneous $\pi^+\pi^-$ or $\pi^0\pi^0$ phonon pair creation where one phonon carries momentum $\tilde{k}$ while the other carries $-\tilde{k}$. The rates $\gamma(\tilde{k})$ computed for typical non-equilibrium configurations, eq. (1), encountered in heavy ion collisions are presented in Figs. IV-VI. The contour lines define surfaces $k_\alpha(\theta_\pi)$ in the pion phase space on which $\gamma(k_\alpha(\theta_\pi), \theta_\pi, \phi_\pi) = \alpha$, where α is a constant. In these figures, α is chosen to be multiples of $0.1\,m_\pi$. The angle θ_π refers to the angle between the pion wavevector $\tilde{k}$ and $\tilde{p}_{cm}$ in eq. (1). The symmetry of $n(\tilde{p})$ in eq. (1) implies that $\gamma(k,\theta,\phi)$ is independent of ϕ and $\gamma(k,\theta) = \gamma(k,\pi-\theta)$.

The regions of phase space where unstable pion modes exist are bounded by critical surfaces $k_c(\theta) = \lim k_\alpha(\theta)$ for $\alpha \to 0^+$. In Figs. IV-VI, we find up to three distinct regions for pionic instabilities. These regions are differentiated from one another by the real parts of the frequencies, $\mathrm{Re}\,\omega_c(\tilde{k})$, for those unstable modes. In region I, $\mathrm{Re}\,\omega_c = 0$;

in region II, Re $\omega_c \approx 0.5\ m_\pi$; in region III, Re $\omega_c \gtrsim m_\pi$. Only the zero frequency modes (I) were considered in Ref. (7). The finite frequency instabilities (II,III) are the analogues of the two beam plasma instabilities[3] that we sought for these non-equilibrium configurations. The phase space for these instabilities is seen to decrease with decreasing p_{cm} and vanishes once the system comes to thermal equilibrium. This is in contrast to the zero frequency instabilities (I) that survive in equilibrated system if $T < T_c(\rho)$ in Fig. I. Further discussion of the differences between instabilities in these regions will be given elsewhere.

The essential feature we want to note here is that the typical phonon pair creation rates $\gamma(\tilde{k})$ are in the range $(0.1 - 0.2)\ m_\pi$. The number of phonons created per unstable mode $\tilde{k}$ is then on the order of one per 1.5×10^{-23} sec. Therefore, there is enough time during the characteristic (thermalization) time $\tau_{th} \sim (2 - 3) \times 10^{-23}$ sec, that specifies the duration of the non-equilibrium phase of the collision, for such pionic instabilities to develop. However, the number of phonons created per mode during this time is small, $\sim 1 - 2$, and thus the term pion condensation is not really appropriate for such systems.

The total number of unstable pion modes is[7]

$$n^\pi_{crit} = \int \frac{3Vd^3k}{(2\pi)^3}\, \theta(\gamma(\tilde{k})) \equiv V/V^\pi_{crit} \qquad , \qquad (17)$$

where V is the volume of nuclear matter where eq. (1) applies. Typically, we estimate $V \approx A_p/\rho_0 = 2A_p\ m_\pi^{-3}$ = volume of projectile nucleus. The critical volume V^π_{crit} defined by eq. (17) is calculated to be in the range $(0.5 - 1.0)\ m_\pi^{-3} \Rightarrow n^\pi_{crit} \approx (2 - 4)\ A_p$. The total number of $\pi^\pm, \pi^0$ phonons that are created in the non-equilibrium phase is then estimated to be $\langle\gamma\rangle\ n^\pi_{crit}\ \tau_{th} \sim 4A_p$.

It is important to note the sensitivity of these estimates to the value of the correlation parameter g in eq. (16). Except for Fig. Vb, all calculations were made with g = 0.5. In Fig. Vb, we took g = 0.6. Compared to Fig. Va, the phase space of instabilities is seen to decrease very much. In fact, the pair production rate per unit volume[7], $\Gamma_{col}/V = \langle\gamma\rangle/V_{crit}$, decreases from $0.18\ m_\pi^4$ to $0.025\ m_\pi^4$ when g is increased from 0.5 to 0.6. For $g \gtrsim 0.65$, no instabilities are found. Therefore, with 20% uncertainties in estimates[2,11] for g, the above calculations with g = 0.5 can be considered only as order of magnitude estimates for $\langle\gamma\rangle$ and V^π_{crit}.

Finally, we note in Figs. IV-VI that the wavenumbers k of unstable modes are typically $\sim(2 - 3)\ m_\pi$. This is of course due to the P-wave nature of the πN interaction in eqs. (3,13). The wavelengths $2\pi/k \sim (3 - 5)$ fm of such modes are then comparable or less than the dimensions of nuclear systems involved in heavy ion collisions.

Therefore, infinite nuclear matter calculations, eqs. (2,16), can be applied to heavy ion collisions only as a result of the large values of k for pionic instabilities.

III. Effects of Pionic Instabilities on the Dynamics

Collective instabilities effect the dynamics in two essential ways: (1) through the growth of collective fields via spontaneous phonon pair creation, and (2) through the modification of two body scattering rates via phonon rather than bare meson exchange. To evaluate the importance of each effect, we first seek a formalism that incorporates them both. A convenient formalism was found in Ref. (7) that involves the calculation of the complex correlation energy density, $\mathcal{M}_{RPA}$, of the system in the Random Phase Approximation. In terms of $\mathcal{M}_{RPA}$, the decay rate Γ of an excited many body state is given by[7]

$$\Gamma = -2V \operatorname{Im} \mathcal{M}_{RPA} \quad . \tag{18}$$

Diagrammatically, $\mathcal{M}_{RPA}$ is the sum of connected ring diagrams as shown in Fig. VII. A general term in this sum consists of a product of n bubbles and n interactions, where each bubble represents $\Pi_{NN} + \Pi_{N\Delta}$ and each interaction represents $\Delta_o + G_c$. Evaluating $\mathcal{M}_{RPA}$, the decay rate per unit volume is found to be[7]

$$\Gamma/V = \operatorname{Re} \int \frac{3d^4k}{(2\pi)^4} \log \varepsilon(\omega,\tilde{k}) \quad , \tag{19}$$

where

$$\varepsilon(\omega,\tilde{k}) = 1 - (\Delta_o + G_c)(\Pi_{NN} + \Pi_{N\Delta}) \tag{20}$$

is the generalized "dielectric" function for the nuclear system. In non-equilibrium systems, the singularities of $\varepsilon(\omega,\tilde{k})$ include overlapping cuts in the ω plane, as seen from eqs. (3c,15), and isolated zeros at $\omega = \operatorname{Re}\omega_c(\tilde{k}) + i\gamma(\tilde{k})$ as found in section II. Equation (19) is then most easily evaluated by first integrating over ω by parts giving[7]

$$\Gamma/V = \int \frac{3d^3k}{(2\pi)^3} \gamma(\tilde{k}) - \frac{1}{2} \int \frac{3d^4k}{(2\pi)^4} \log\left(1 - 4\, I(\omega) I(-\omega) |\Delta_c|^2\right)$$

$$\equiv \Gamma_{col}/V + \Gamma_{scat}/V \quad , \tag{21}$$

where

$$I(\omega,\tilde{k}) = I_{NN}(\omega,\tilde{k}) + I_{N\Delta}(\omega,\tilde{k}) \tag{22}$$

is defined via eqs. (3c,15), and

$$\Delta_c(\omega,\tilde{k}) = (\Delta_o(\omega,\tilde{k}) + G_c(\tilde{k}))/\varepsilon(\omega,\tilde{k}) \tag{23}$$

is the correlated pion propagator. Equation (21) allows us to calculate the growth rate of collective fields via Γ_{col} and the scattering rate Γ_{scat} in non-equilibrium systems, eq. (1). A further decomposition of Γ_{scat} is possible noting that the integrand vanishes unless $I(\omega)I(-\omega) \neq 0$. Then

$$\Gamma_{scat} = \Gamma_{NN} + \Gamma_{N\Delta} + \Gamma_{\Delta\Delta} \tag{24}$$

where

$$\begin{Bmatrix} \Gamma_{NN} \\ \Gamma_{N\Delta} \\ \Gamma_{\Delta\Delta} \end{Bmatrix} = \int \frac{3Vd^4k}{(2\pi)^4} \begin{Bmatrix} 2\ I_{NN}(\omega)I_{NN}(-\omega) \\ 4\ I_{NN}(\omega)I_{N\Delta}(-\omega) \\ 2\ I_{N\Delta}(\omega)I_{N\Delta}(-\omega) \end{Bmatrix} P(\omega,k)\,|\Delta_o + G_c|^2 \quad , \tag{25}$$

and the polarization form factor P is

$$P(\omega,\tilde{k}) = \frac{-\log(1 - 4\,I(\omega)\ I(-\omega)\,|\Delta_c|^2)}{4\,I(\omega)\ I(-\omega)\,|\Delta_o + G_c|^2} \quad . \tag{26}$$

Γ_{NN} is the effective elastic $NN \to NN$ scattering rate, while $\Gamma_{N\Delta}$ and $\Gamma_{\Delta\Delta}$ are the effective inelastic $NN \to N\Delta$ and $NN \to \Delta\Delta$ rates in the medium. In the low density limit, $\Pi_{NN} + \Pi_{N\Delta} \to 0 \Rightarrow P(\omega,\tilde{k}) \to 1$, and Γ_{ij} reduce to rates calculated with free space cross sections, $d\sigma^o$, i.e.

$$\Gamma_{ij}/V \xrightarrow[\rho\to 0]{} \Gamma^o_{ij}/V \equiv \rho^2 < \sigma^o_{NN \to ij}\ v_{rel} > \quad . \tag{27}$$

Diagrammatically, only the third term in Fig. VII contributes to Γ_{ij} in the low density limit, giving $d\sigma^o \propto |\Delta_o + G_c|^2$. At high densities effective two body (elastic and inelastic) cross sections, $d\sigma_{eff}$, can be derived[7] from eq. (25) giving

$$d\sigma_{eff} = P(\omega,\tilde{k})\ d\sigma^o \quad , \tag{28}$$

where $(\omega,\tilde{k})$ are the energy-momentum transfers in the process. Therefore, $P(\omega,\tilde{k})$ contains the density and configuration dependence of the effective cross sections in the medium. For systems close to equilibrium, P reduces to[7]

$$P(\omega,\tilde{k}) \approx \frac{1}{|\varepsilon(\omega,\tilde{k})|^2} \quad , \tag{29}$$

as is found in the kinetic theory of plasmas.[12] The important point to note about eq. (28) is that the existence of collective instabilities implies that there exist certain critical values of $(\omega_c, \tilde{k}_c)$ such that $P(\omega_c, \tilde{k}_c) \to \infty$ and hence $d\sigma_{eff} \to \infty$ if the energy-momentum transfer $(\omega_c, \tilde{k}_c)$ is kinematically allowed. This is known as critical scattering phenomena and is extensively discussed in Ref. (7). Thus the presence of the polarization factor in eq. (28) leads to enhanced scattering rates if instabilities are present.

As an example of the kind of enhancements pionic instabilities lead to, $P(\omega,\tilde{k}) = d\sigma_{eff}/d\sigma^o$ is plotted in Fig. VIII for $p_{cm} = 4m_\pi$ in eq. (1). This figure is taken from Ref. 7 and corresponds to the elastic $(\omega = 0)$ scattering of a nucleon of momentum $\tilde{p}_{cm}$ with another of momentum $-\tilde{p}_{cm}$ in the medium. Kinematically, $\tilde{k}$ is constrained by $k = 2\, p_{cm} \cos\theta_\pi$. Logarithmic divergencies of $d\sigma_{eff}$ at $k \approx 1.5$ and $2.0\ m_\pi$ arise when kinematically allowed values of (k,θ_π) lie on the boundary of region I of unstable pion modes (see Fig. XIV of Ref. 7 and Fig. Va here). Figure VIII illustrates then critical scattering phenomena for large momentum transfers that arise as a result of pionic instabilities.

The integrated scattering rates are given in Table I for a variety of lab kinetic energies, $T_L \sim (0.4 - 1.5)$ GeV/nucleon. It must be emphasized that the spirit of these calculations is to obtain only order of magnitude estimates of the effects of pionic instabilities on these rates. We cannot expect to predict absolute rates with such a simple model. Nevertheless, the ratios of effective rates Γ^{eff}_{ij} to free rates Γ^o_{ij} do indicate the magnitude of enhancements that can arise due to collective phenomena. The rates in table I were obtained by integrating numerically eq. (25) up to momentum transfers $k = 8\ m_\pi$. The free rates Γ^o_{ij} were obtained from eq. (25) by setting $P(\omega,\tilde{k}) = 1$. To set a scale for the absolute magnitudes of Γ_{ij}, note that a 20 mb cross section in eq. (27) would give $\Gamma_{ij}/V \approx 0.25\ m_\pi^4$. The essential point to note in tables IA,B is that both the elastic and inelastic scattering rates are enhanced by factors $\sim (2 - 4)$ due to pionic instabilities. Further details of these calculations will be given elsewhere.

IV. Summary

Model calculations of dense, excited nuclear matter expected in heavy ion collisions indicate that in both thermal[4] and non-equilibrium[7] extremes pionic instabilities can be expected. The typical excitation energies involved in these high energy ($\sim$ 1 GeV/nuc) collisions are not too large to prevent such instabilities. Furthermore, the spontaneous phonon pair creation rates $\gamma(\tilde{k})$ were shown to be sufficiently large for these instabilities to develop during the short collision times. In the non-equilibrium case finite frequency instabilities (regions II,III) were found as well as zero frequency (condensate) instabilities (region I). The total $\pi^+\pi^-$ and $\pi^o\pi^o$ phonon pair creation rate $\Gamma_{col} = \langle\gamma\rangle\, V/V^\pi_{crit} \equiv \Gamma_o + \Gamma_{\pi'}$ is given in table IC, with Γ_o being the

rate for zero frequency pairs and Γ_{π}, being the rate for finite frequency pairs. We noted also the short wavelengths $2\pi/k_c \sim (3-5)$ fm of these pion modes as being essential for such instabilities to develop in the finite size nuclear systems involved.

Then through the calculation of the complex correlation energy, the effect of pionic instabilities on the dynamics was studied. The main result is that critical scattering phenomena leads to enhancements of both elastic and inelastic scattering rates by factors $\sim 2-4$. We can now assess the relative importance of the two effects mentioned at the beginning of section III. The ratio $\Gamma_{col}/\Gamma_{scat}$ of rates in eq. (21) provides a measure of which effect dominates. This ratio is given table IC. Note that $\Gamma_{col}/\Gamma_{scat} < 1$ in all cases indicating that the scattering rates are greater than the growth rates of collective fields. Therefore, the dynamics is dominated by two body collisions involving density dependent interactions, eq. (28). The reduction by 2 - 4 of the effective nucleon mean free path in the medium is therefore expected to lead to more rapid thermalization, indicating that a hydrodynamic description[5,6,13] of the dynamics would be appropriate.[7]

Finally, we comment on the implication of the enhancement of $\Gamma_{N\Delta}^{eff}$ in the medium in connection with real pion production. It is tempting to assume that a factor of 2 enhancement of the $NN \to N\Delta$ rate would lead to twice as many pion being observed in the lab. However, the final number of pions observed depends not only on the production rate $\Gamma_{N\Delta}$ but also sensitively on the absorption rates of pions. Therefore, to estimate real pion production rates, the effects of pionic instabilities on pion absorption rates must also be investigated. Such an investigation is currently in progress.

References

*This work was done with support from the U.S. Energy Research and Development Administration.

1. A. B. Migdal, O. A. Markin, I. I. Mishustin, Sov. Phys. JETP 39 (1974) 212

2. G. E. Brown, W. Weise, Phys. Reports 27C (1976) 1

3. O. Buneman, Phys. Rev. 115 (1959) 503

4. V. Ruck, M. Gyulassy, W. Greiner, Z. Physik A277 (1976) 391

5. H. G. Baumgart, J. U. Schott, Z. Sakamoto, E. Schopper, H. Stöcker, J. Hofmann, W. Scheid, W. Greiner, Z. Physik A273 (1975) 359

6. M. I. Sobel, P. J. Siemens, J. P. Bondorf, H. A. Bethe, Nucl. Phys. A251 (1975) 502

7. M. Gyulassy, W. Greiner, Ann. Phys. (in press)

8. W. A. Mann et al., Phys. Rev. Lett. 31 (1973) 844

9. P. A. Schreiner, F. V. Hippel, Phys. Rev. Lett. 30 (1973) 339

10. G. E. Brown, W. Weise, Phys. Rep. C22 (1975) 279

11. S. O. Bäckman, W. Weise, Phys. Lett. 55B (1975) 1;
G. Baym, G. E. Brown, Nucl. Phys. A247 (1975) 395

12. H. W. Wyld, D. Pines, Phys. Rev. 127 (1962) 1851

13. A. A. Amsden, F. H. Harlow, J. R. Nix, Los Alamos preprint LA-UR-77-31 (1977)

Table Caption:

I. Collective Γ_{col} and scattering Γ_{ij} rates in non-equilibrium nuclear matter at various lab energies T_L. The $NN \to NN$ rates (A), $NN \to N\Delta$ rates (B), and spontaneous $\pi^+\pi^-$, $\pi^0\pi^0$ phonon pair creation rates (C) were calculated with eqs. (21,25). The enhancements of the scattering rates due to pionic instabilities are given by σ_{eff}/σ_0 in A and B. The ratio $\Gamma_{col}/\Gamma_{scat}$ in C measures the importance of phonon pair production as compared to the modification of the scattering rates on the dynamics.

Figure Captions

I. Range of densities and temperatures where pion condensation is likely (shaded). T_{crit} is taken from Ref. (4) for $g = 0.5$. Curves AB and BC illustrate the compression and decompression phases in heavy ion collisions.

II. Initial non-equilibrium momentum distribution in heavy ion collisions.

III a) Pion propagator Δ in a nuclear medium.

b) Polarization operator Π including nucleon particle-hole and Δ_{33} - nucleon hole intermediate states as well as correlations.

IV. a) Contour plot for the rates $\gamma(k_\pi, \theta_\pi)$ of spontaneous $\pi^+\pi^-$ or $\pi^0\pi^0$ phonon pair creation in non-equilibrium nuclear matter, eq. (1), for $p_{cm} = 2.0\ m_\pi$. Contours correspond to multiples of $0.1\ m_\pi (\approx 2 \times 10^{22}\ sec^{-1})$. The angle θ_π is that between $\tilde{k}_\pi$ and $\tilde{p}_{cm}$. Zero frequency (Re $\omega_c = 0$) pionic instabilities occur in region I. Finite frequency (Re $\omega_c \neq 0$) instabilities occur in regions II, III.

b) Same as IVa but for $p_{cm} = 3.0\ m_\pi$.

V. a) Same as IVa but for $p_{cm} = 4.0\ m_\pi$.

b) Same as Va but with large correlation parameter $g = 0.6$.

VI. a) Same as IVa but for $p_{cm} = 5.0\ m_\pi$.

b) For $p_{cm} = 6.0\ m_\pi$.

VII. Series of ring diagrams included in the Random Phase Approximation for the correlation energy density $\mathcal{M}_{RPA}$ in eq. (18).

VIII. Ratio of the effective $d\sigma_{eff}$, to the free, $d\sigma_o$, elastic ($NN \to NN$) differential cross sections as a function of momentum transfer k as calculated via eq. (28). (Taken from Fig. XIb of Ref. 7). This illustrates critical scattering phenomena due to pionic instabilities.

Table I

A. Elastic Scattering Rates

T_L (GeV/N)	p_{cm}/m_π	$\Gamma^{eff}_{NN}/V(m_\pi^4)$	$\Gamma^{o}_{NN}/V(m_\pi^4)$	$\sigma^{el}_{eff}/\sigma^{el}_{o}$
0.38	3	0.37	0.09	4.1
0.67	4	0.31	0.08	3.9
1.04	5	0.27	0.07	3.9
1.50	6	0.22	0.06	3.7

B. Inelastic Scattering Rates

T_L (GeV/N)	p_{cm}/m_π	$\Gamma^{eff}_{N\Delta}/V(m_\pi^4)$	$\Gamma^{o}_{N\Delta}/V(m_\pi^4)$	$\sigma^{in}_{eff}/\sigma^{in}_{o}$
0.38	3	0.24	0.06	4.0
0.67	4	0.58	0.28	2.1
1.04	5	0.72	0.42	1.7
1.50	6	0.64	0.39	1.6

C. Collective Rates

T_L (GeV/N)	p_{cm}/m_π	$\Gamma_{col}/V(m_\pi^4)$	$\Gamma_{\pi'}/\Gamma_o$	$\Gamma_{col}/\Gamma_{scat}$
0.38	3	0.21	0.47	0.34
0.67	4	0.18	0.47	0.20
1.04	5	0.25	0.50	0.25
1.50	6	0.59	3.20	0.69

Fig. 1

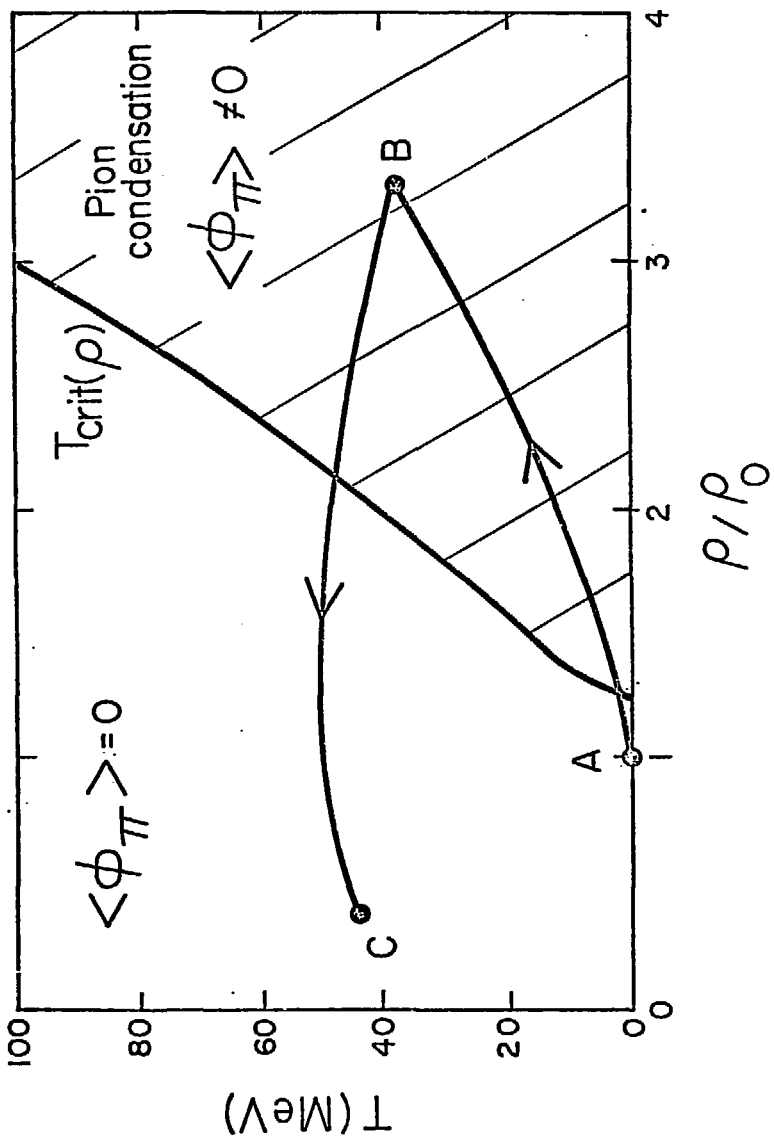

XBL776-1092

Fig. II

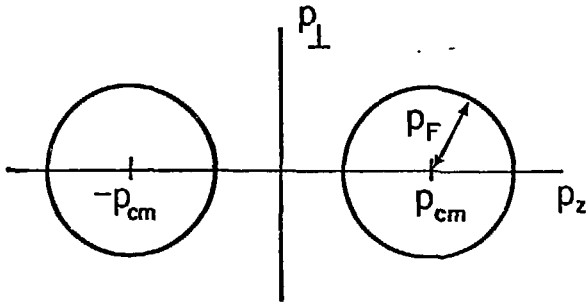

XBL776-1091

Fig. III

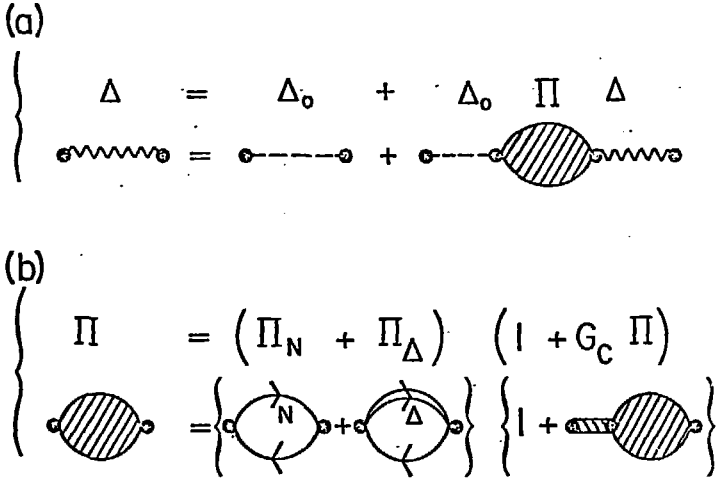

XBL776-1090

Fig. IV

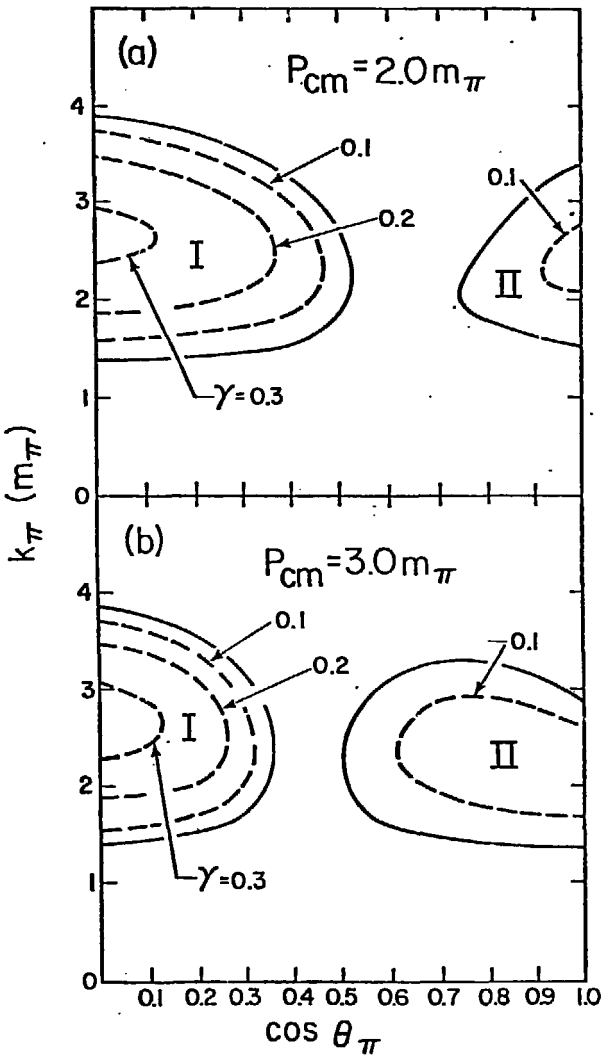

XBL 776-1094

Fig. V

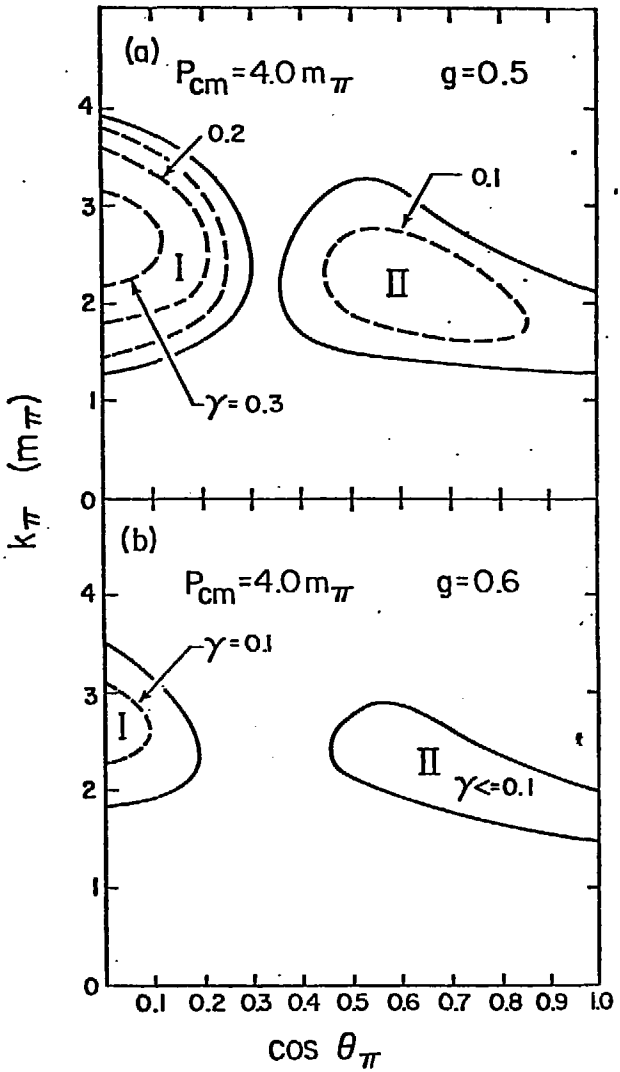

XBL 776-1093

Fig. VI

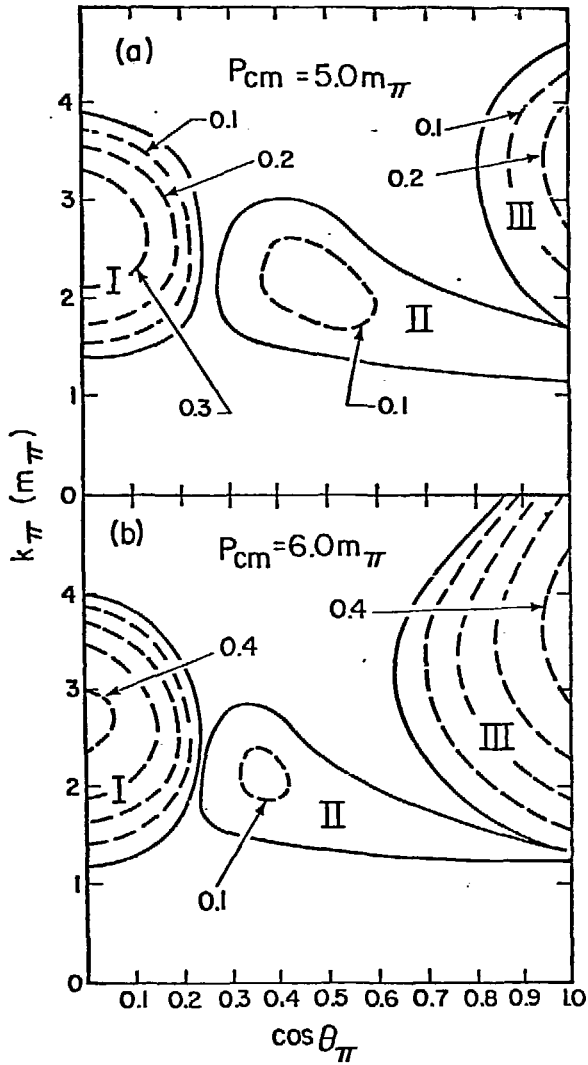

XBL776-1095

Fig. VII

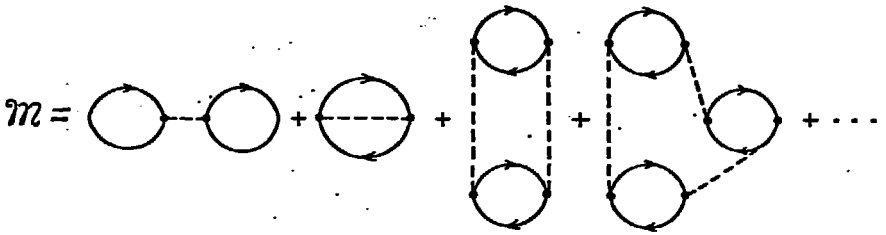

Fig. VIII

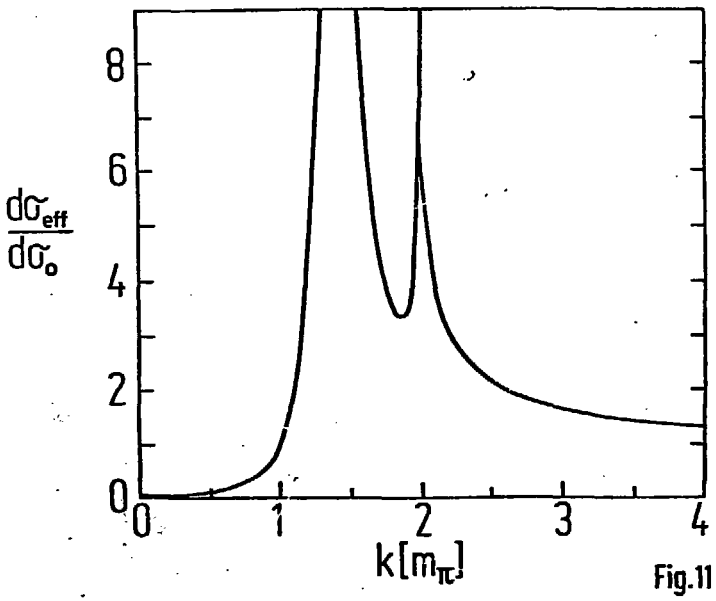

Fig.11

XBL 772-7475